Chaos as Irregular Hopping between Unstable Periodic Orbits and Its Network Representation

Syuji Miyazaki[1*] and Yusuke Higuchi[2**]

[1] *Graduate School of Informatics, Kyoto University, Kyoto 606-8501, Japan*
[2] *Faculty of Engineering, Kyoto University, Kyoto 606-8501, Japan*
[*] *E-mail address: syuji@acs.i.kyoto-u.ac.jp*

(Received April 14, 2013; Accepted May 27, 2013)

Based on a matrix representation of the generalized Frobenius-Perron operator describing large-deviation statistics of local expansion rates of one-dimensional chaotic map, directed graphs are constructed. Its network statistics reflect characteristic fluctuation in the vicinity of a specific bifurcation. In this treatment, chaos can be described as an irregular switching between finite specific unstable periodic orbits. Type-I intermittency is analyzed for the solvable Shobu-Ose-Mori map and the logistic map. Solvable irreducible and approximate redundant partitions are constructed to obtain directed graphs and degree distributions. The output degree distribution obtained from a redundant partition slightly fluctuates around that obtained from a irreducible partition in the case of a tent map. It is shown that the output degree distribution is a good candidate to capture characteristics of Type-I intermittency.

Key words: Deterministic Chaos, Complex Network, Type-I Intermittency, Degree Distribution, Unstable Periodic Orbit

1. Introduction

Large-deviation statistics or statistical thermodynamics of temporal fluctuations of the local expansion rate have been studied in the research area of chaos (Mori and Kuramoto, 1998; Gaspard, 1998). Starting from a matrix representation of the generalized Frobenius-Perron operator which is a fundamental operator of large-deviation statistics, we construct a directed map as a description of chaos and its network statistics such as output degree distribution. There exist various studies analyzing relationship between chaos and graph, or between chaos and coding in a different perspective (Bollt *et al.*, 1997; Zhang and Small 2006; Zhang *et al.*, 2008).

We will also show an idea that the nodes of the directed graph can be corresponded to finite specific unstable periodic orbits (UPOs) and that chaos can be described as an irregular switching between such finite specific UPOs among the countable infinite number of UPOs.

In the second section, we explain the Frobenius-Perron operator and its generalization. Our basic idea is described in Section 3. A solvable model of the Type-I intermittency is analyzed in Section 4. Numerical results for the logistic map, the parameter of which corresponds to Type-I intermittency is shown in Section 5. The final section is devoted to concluding remarks.

**Present address: NS Solutions, NBF Shinkawa Building 20-15, Shinkawa 2-chome, Chuo-ku, Tokyo 104-8280, Japan.

2. Frobenius-Perron Operator and Its Generalization

A chaotic one-dimensional map $x_{n+1} = F(x_n)$ yields a chaotic sequence of $\{x_n\}$, whose distribution functions at time n, $\rho_n(x)$, evolves in the course of time, once an ensemble of initial values $\{x_0\}$ is given. The distribution is also written (Fujisaka and Inoue, 1987) as

$$\rho_n(x) \equiv \langle \delta(x_n - x) \rangle, \tag{1}$$

where $\langle \cdots \rangle$ denotes an average taken over various initial values x_0. Its temporal evolution is given by

$$\rho_{n+1}(x) = \int_0^1 \delta(F(y) - x)\rho_n(y)dy \equiv \mathcal{H}\rho_n(x) \tag{2}$$

where $\mathcal{H}$ is a Frobenius-Perron operator for an arbitrary function $G(x)$ of x explicitly given by

$$\mathcal{H}G(x) = \sum_j \frac{G(y_j)}{|F'(y_j)|}. \tag{3}$$

The sum is taken over all solutions y_j satisfying $F(y_i) = x$.

A dynamics quantity $u[x]$ such as local expansion rate $u[x] = \log|F'(x)| = \log|\frac{dF(x)}{dx}|$ fluctuates and distributes. In the framework of large-deviation formalism, the Frobenius-Perron operator is generalized as

$$\mathcal{H}_q G(x) = \mathcal{H}[e^{qu[x]}G(x)] = \sum_k \frac{e^{qu[y_k]}G(y_k)}{|F'(y_k)|}, \tag{4}$$

where q is a real parameter and the sum is taken over all solutions y_j satisfying $F(y_i) = x$.

In the next section, $\mathcal{H}_q$ is represented by a matrix H_q for a piecewise-linear chaotic map.

3. Simple Example

We consider the following piecewise-linear map h from unit interval $I = [0,1]$ to I

$$h(x) = Ax + 1 - \frac{1}{B}\left(x \in I_1 = \left[0, 1 - \frac{1}{B}\right)\right), \quad (5)$$

$$h(x) = -B(x-1)\left(x \in I_2 = \left[1 - \frac{1}{B}, 1\right]\right), \quad (6)$$

where the parameter B satisfies $B \geq 1$ and the parameter A is given by $A = \frac{1}{B-1}$. It should be noted that two intervals I_1 and I_2 construct a Markov partition of I in the following sense: $h(I_1) = I_2$ and $h(I_2) = I_1 \cup I_2$.

On the basis that two definition functions which are equal to unity, zero otherwise, for $x \in I_1$ or $x \in I_2$, the Frobenius-Perron operator $\mathcal{H}_0$ is represented by the following matrix H_0

$$H_0 = \begin{pmatrix} 0 & \frac{1}{B} \\ \frac{1}{A} & \frac{1}{B} \end{pmatrix} = \begin{pmatrix} 0 & 1 \\ 1 & 1 \end{pmatrix}\begin{pmatrix} \frac{1}{A} & 0 \\ 0 & \frac{1}{B} \end{pmatrix}. \quad (7)$$

Let us consider a piecewise-constant dynamical quantity u, which takes two values $u(I_1)$ or $u(I_2)$ for $x \in I_1$ or $x \in I_2$, respectively. In the same way, the generalized Frobenius-Perron operator $\mathcal{H}_q$ is given by the following matrix H_q

$$H_q = \begin{pmatrix} \frac{\exp(qu(I_1))}{A} & \frac{\exp(qu(I_2))}{B} \\ 0 & \frac{\exp(qu(I_2))}{B} \end{pmatrix} \quad (8)$$

$$= \begin{pmatrix} 0 & 1 \\ 1 & 1 \end{pmatrix}\begin{pmatrix} \frac{\exp(qu(I_1))}{A} & 0 \\ 0 & \frac{\exp(qu(I_2))}{B} \end{pmatrix}. \quad (9)$$

When we take the local expansion rate $\log|h'(I_1)| = \log A$ or $\log|h'(I_2)| = \log B$ as u, H_1 is given by the following matrix whose components are either zero or unity

$$H_1 = \begin{pmatrix} 0 & 1 \\ 1 & 1 \end{pmatrix}, \quad (10)$$

which can be regarded as a adjacency matrix standing for the relations $h(I_1) = I_2$ and $h(I_2) = I_1 \cup I_2$. One can also draw a directed graph consisting of two nodes corresponding to I_1 and I_2. The unstable fixed point (UPO) satisfying $-b(x^{(1)} - 1) = x^{(1)}$ is given by $x^{(1)} = \frac{B}{B+1} \in I_2$. The unstable periodic point $x_1^{(2)} \in I_1$ satisfying $-B(\frac{1}{B-1}x_1^{(2)} + 1 - \frac{1}{B} - 1) = x_1^{(2)}$ is given by $x_1^{(2)} = \frac{2B^2-2B+1}{B(2B-1)}$, which is mapped to $x_2^{(2)} = \frac{B-1}{2B-1} \in I_2$, which is mapped back to $x_1^{(2)}$. The intervals I_1 and I_2 respectively contain $x_1^{(2)}$ and $x^{(1)}$ as the shortest UPO.

These two shortest UPOs appears as characteristic frequencies in the order-q power spectrum and in the order-q correlation function (Fujisaka and Shibata 1991), which is generalized versions in the framework of large-deviation statistics. Two eigenvalues $\upsilon_q^{(\pm)}$ are given by

$$\upsilon_q^{(\pm)} = \frac{b^{q-1} \pm \sqrt{B^{2q-2} + 4A^{q-1}B^{q-1}}}{2}, \quad (11)$$

the ratio of which is given by

$$\frac{\upsilon_q^{(-)}}{\upsilon_q^{(+)}} = -1 + \frac{B^{q-1} + \sqrt{B^{2q-2} + 4A^{q-1}B^{q-1}}}{2A^{q-1}} \quad (12)$$

The decay rate of the order-q correlation function is given by $\Re[\log \frac{\upsilon_q^{(-)}}{\upsilon_q^{(+)}}]$, and the angular frequency of periodic component of the order-q power spectrum is given by $\Im[\log \frac{\upsilon_q^{(-)}}{\upsilon_q^{(+)}}]$. The fact that the ratio $\frac{\upsilon_q^{(-)}}{\upsilon_q^{(+)}}$ approaches zero for $q \to \infty$ and -1 for $q \to -\infty$ implies a constant signal and a period-2 signal due to $-1 = \exp(i\pi)$, which are induced by the above-mentioned unstable fixed point and unstable periodic points with period-2. It should be noted that $\log \upsilon_0^{(+)}$ is equal to the Lyapunov exponent, and $\log \upsilon_1^{(+)}$ the topological entropy. In the framework of large-deviation statistics, the topological entropy is a weighted average of the local expansion rate, the larger values of which takes the more weight.

According to our standpoint of view, this chaotic system is described as an irregular switching motion between a unstable fixed point and a unstable period-2 motion, although the countable infinite numbers of UPOs exist. This switching motion can be represented by the above-mention 2×2 adjacency matrix.

4. Shobu-Ose-Mori Map as a Solvable Model of the Type-I Intermittency

In the vicinity tangent bifurcation point with a suitable reinjection mechanism, where the pair of stable and unstable fixed points are about to be generated, the Type-I intermittency occurs. A solvable map is introduced by Shobu, Ose and Mori (1984),which will be abbreviated as SOM map in the following. It is explicitly given by

$$f(x) = \begin{cases} \alpha x + 0.2 & (0 \leq x \leq \gamma), \\ \alpha^{-1}(x - 0.8) + 1 & (\gamma \leq x \leq 0.8), \\ -\beta^{-1}(x-1) & (0.8 \leq x \leq 1), \end{cases} \quad (13)$$

where real positive parameters α, β and γ satisfy $0.6 < \alpha < 1$, $\beta = 0.2$, $\gamma = 0.8/(1+\alpha)$. At $\alpha = 0.6$, the bifurcation occurs, and the SOM map has a *channel* in the vicinity of $x \sim \gamma$ for $\alpha \gtrsim 0.6$ as shown in Fig. 1. The time series of x are shown in Fig. 2. The intermittent behavior consists of the laminar part $0 < x < 0.8$ and the burst part $0.8 < x$. Markov partitions are obtained at specific values of α, $\alpha = \alpha_m$ $(m = 3, 4, \cdots)$, satisfying

$$\alpha^{m+1} + \alpha^m - 5\alpha + 3 = 0, \quad (14)$$

where the unit interval $[0,1]$ can be divided into $2m+1$ subintervals at $\alpha = \alpha_m$. The edge of the subinterval is given by iteration starting from $x_0 = 0$, $x_1 = f(x_0)$, $x_2 = f(x_1)$, $\cdots$, $x_{2m} = f(x_{2m-1}) = 0.8$, and $x_{2m+1} = f(x_{2m}) = 1$, which is shown in Fig. 3 for $\alpha = \alpha_4 \simeq 0.665$. Let subintervals be $I_1 = [x_0, x_1]$, $I_2 = [x_1, x_2]$, $\cdots$, $I_{2m+1} = [x_{2m}, x_{2m+1}]$. For $1 < i < 2m$, I_i is mapped to I_{i+1}, and I_{2m+1} to the whole interval $[0,1]$.

In this map, the local expansion rate is equal to either of three values $\log\alpha$, $-\log\alpha$ and $\log\beta$. The large-deviation statistics are obtained from H_q, ij components of which $(H_q)_{i,j}$ are explicitly given by

$$(H_q)_{i,j} = \begin{cases} \alpha^{q-1} & (i+1 = j, i = 1, \cdots, m), \\ \alpha^{1-q} & (i+1 = j, i = m+1, \cdots, 2m), \\ \beta^{1-q} & (i = 2m+1), \\ 0 & (\text{otherwise}). \end{cases} \quad (15)$$

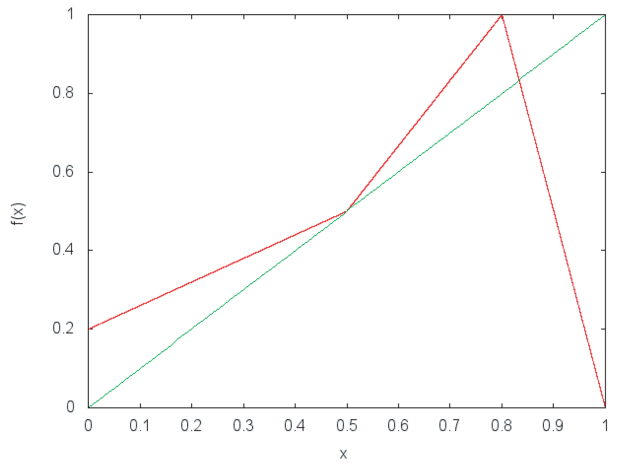

Fig. 1. SOM map ($\alpha = 0.60001$).

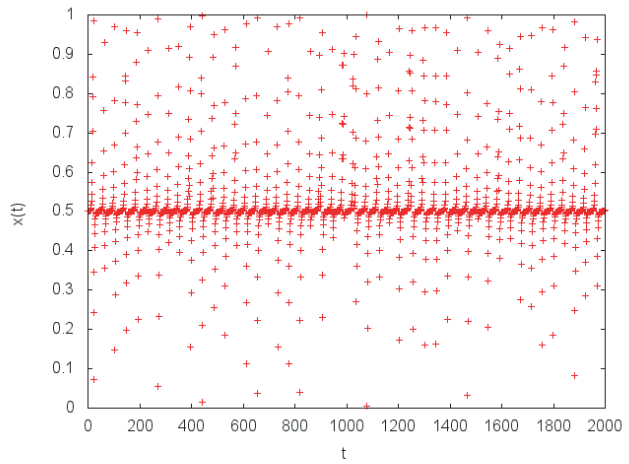

Fig. 2. Time series of the SOM map ($\alpha = 0.60001$).

For $q = 1$, we have

$$(H_1)_{i,j} = \begin{cases} 1 \ (i+1 = j \text{ or } i = 2m+1) \\ 0 \ (\text{otherwise}) \end{cases} \tag{16}$$

Regarding H_1 as an adjacency matrix, we can draw a directed graph. The burst part I_{2m+1} mapped to the whole $2m+1$ subintervals yields output degree $2m+1$, and the laminar part I_i mapped to the right neighbor subinterval I_{i+1} yields output degree 1, and the number of such subintervals is equal to $2m$, so that output degree distribution $P(d)$ is given by

$$P(d) = \frac{2m}{2m+1}\delta_{d,1} + \frac{1}{2m+1}\delta_{d,2m+1}, \tag{17}$$

where $\delta_{i,j}$ denotes Kronecker delta. The directed graph corresponding to Type-I intermittency is thought to consist of many small-output-degree nodes and a few large-output-degree nodes, which will be confirmed for the logistic map in the subsequent section.

The burst part I_{2m+1} has a unstable fixed point as the shortest UPO in this subinterval. In the laminar part, one of the unstable period-2 periodic points visits I_{2m} and I_{2m+1}, which is the shortest UPO in I_{2m}. In the same way, one of

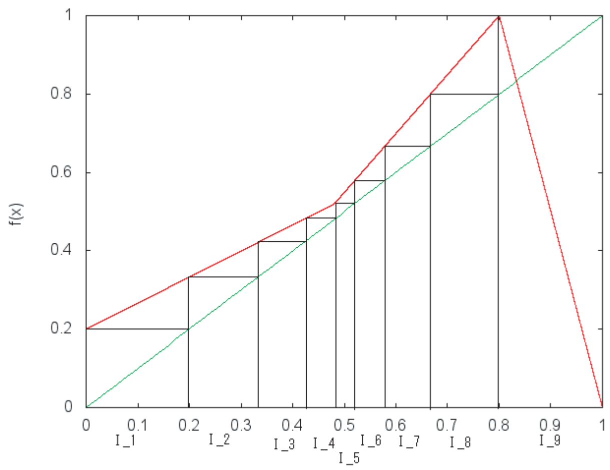

Fig. 3. Markov partition at $\alpha = \alpha_4 \simeq 0.665$.

the unstable period-3 periodic points visits I_{2m-1}, I_{2m} and I_{2m+1}, which is the shortest UPO in I_{2m-1}. The shortest UPO in I_k corresponds recursively to UPO with period-$(2m+2-k)$. Type-I intermittency of the SOM map can be described by a switching motion only between period-1, period-2, $\cdots$, period-$(2m+1)$ UPOs among countable infinite number of UPOs. It should be noted that the period-1 to period-$2m+1$ UPOs appear as delta-function-like lines in the power spectrum as shown in the preceding study (Shobu, Ose and Mori 1984).

5. Type-I Intermittency of the Logistic Map

We consider the logistic map in this section, which is explicitly given by

$$g(x) = ax(1-x) \ (x \in [0,1]). \tag{18}$$

where real parameter a satisfy $0 \le a \le 4$. In the chaotic regions for $a \ge 3.5699456\cdots$, a period-3 window in the vicinity of $a = 3.84$ is remarkable in the bifurcation diagram. This window locates between the tangent bifurcation point $a = a^{(3)}$ and the band crisis point. Every third iteration $g^3(x) = g \circ g \circ g(x)$ has three *channels* just before the tangent bifurcation point, at which period-3 points are generated.

In order to construct Markov partitions approximately, if an initial point x_0 is mapped into $[x_0 - \epsilon, x_0 + \epsilon]$ after n steps of the mapping function $g^3(x)$, we replace x_0 and x_n by $\frac{x_0+x_n}{2}$, and approximated periodic points $\frac{x_0+x_n}{2}$, x_1, x_2, $\cdots$, x_{n-1} with period-n are used as both endpoints of the subintervals $I_1, I_2, \cdots, I_n$ constructing Markov partition. We set $\epsilon = 0.001$ in the following, and the recurrence time n is assumed to be much longer than the average laminar duration. Around $a = 3.828$, the average laminar duration is nearly equal to 50 steps, we will consider 100 or more iterations of $g^3(x)$ as n.

In order to obtain a matrix representation of the generalized Frobenius-Perron operator, the mapping function is replaced to a piecewise-linear function between the above-mentioned endpoints, so that H_q is equal to $|\frac{dg^3(I_j)}{dx}|^{q-1}$, if I_j is mapped to I_i, $H_q = 0$ otherwise. Although the original local expansion rate $\log|\frac{dg^3(x)}{dx}|$ varies continuously, the

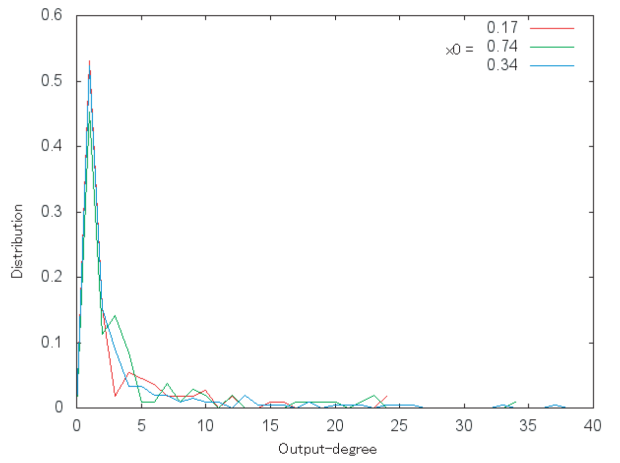

Fig. 4. Output degree distribution at $a = 3.828$ for different initial values $x_0 = 0.17$ ($n = 111$), 0.74 ($n = 106$), 0.34 ($n = 210$).

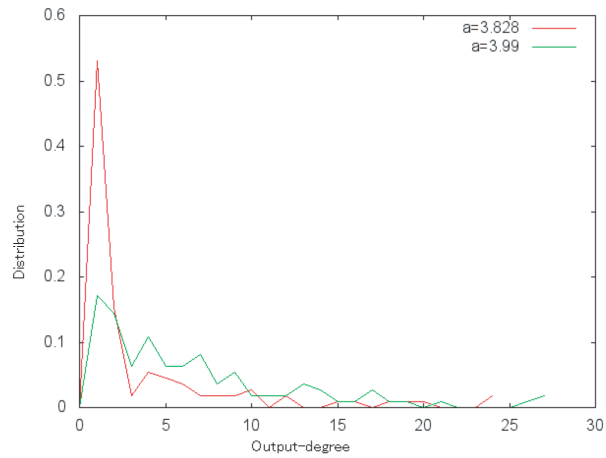

Fig. 6. Output degree distributions at $a = 3.828$ (red) and at $a = 3.99$ (green).

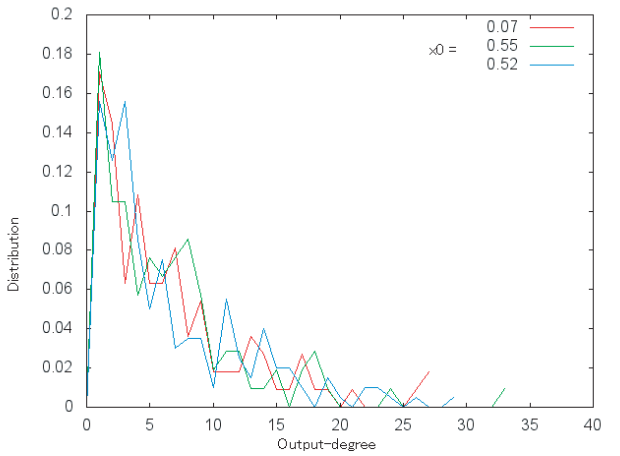

Fig. 5. Output degree distribution at $a = 3.99$ for different initial values $x_0 = 0.07$ ($n = 112$), 0.55 ($n = 105$) and 0.52 ($n = 212$).

local expansion rate takes either of n values $\log|\frac{dg^3(I_1)}{dx}|$, $\log|\frac{dg^3(I_2)}{dx}|$, $\cdots$, $\log|\frac{dg^3(I_n)}{dx}|$ by our approximation. The ij component of H_1 is equal to unity, if I_j is mapped to I_i, zero otherwise. Regarding H_1 as an adjacency matrix, we can draw a directed graph. We compare two graphs at $a = 3.828$, where Type-I intermittency is observed, and at $a = 3.99$, where no specific bifurcation exists in the vicinity.

Figure 4 depicts the output degree distribution at $a = 3.828$ for different initial values $x_0 = 0.17$ ($n = 111$), 0.74 ($n = 106$) and 0.34 ($n = 210$). Figure 5) depicts the output degree distribution at $a = 3.99$ for different initial values $x_0 = 0.07$ ($n = 112$), 0.55 ($n = 105$) and 0.52 ($n = 212$). From above two figures, we see less remarkable differences in the output degree distribution for different choice of the initial value.

Output degree distributions at $a = 3.828$ and at $a = 3.99$ is all together shown in Fig. 6, in which the initial value $x_0 = 0.17$ ($n = 111$) is used at $a = 3.828$, and $x_0 = 0.07$ ($n = 112$). From this distribution, we see a concentration of small output degree is observed in the case of the Type-I intermittency $a = 3.828$, and a broader distribution is observed when no specific bifurcation point is located $a = 3.99$. Note that the output degree distribution has nonzero value between 1 and the average value of the laminar duration $\simeq 50$ in Fig.4 even for the longer period of the approximate UPOs, the values of which are distributed between 106 and 210.

6. Concluding Remarks

We reconsider the piecewise-linear map described in Section 3. For the sake of simplicity, we set $A = 1$ and $B = 2$ in the following. The map $h(x)$ consists of the left part $h(x) = L(x) = x + 1/2$ ($x \in I_1 = [0, 1/2)$) and the right part $h(x) = R(x) = -2x + 2$ ($x \in I_2 = [1/2, 1]$). We will consider the first three UPOs satisfying $x = RL(x)$, $x = R^3L(x)$ and $x = R^4L(x)$. The period-2 UPOs $x = RL(x)$ is explicitly given by $x = 1/3$ followed by $L(1/3) = 5/6$, which is mapped backed to $RL(1/3) = 1/3$. The initial value $x = 1/3 + \epsilon/2$ ($0 < \epsilon \ll 1$) is mapped to $RL(1/3 + \epsilon/2) = 1/3 - \epsilon$, so that the numerical procedure described in Section 5 can be applied to this map. We choose the initial value $x^* \in [1/3 - \epsilon/2, 1/3 + \epsilon/2]$. The two points $x = x^*$ and $x = L(x^*)$ with the edge points $x = 0, 1$ and the boundary point $x = 1/2$ between I_1 and I_2 divide the unit interval into four subintervals. The adjacency matrix is given by

$$\begin{pmatrix} 0 & 0 & 0 & 1 \\ 0 & 0 & 1 & 0 \\ 1 & 0 & 1 & 0 \\ 0 & 1 & 1 & 0 \end{pmatrix},$$

and the largest eigenvalue is equal to the golden mean $\frac{1+\sqrt{5}}{2}$. The output degree distribution is given by $P(d) = \frac{3}{4}\delta_{d,1} + \frac{1}{4}\delta_{d,3}$.

The period-3 UPOs satisfying $x = R^2L(x)$ is given by $x = 0$, $L(0) = 1/2$ and $RL(1/2) = 1$, which is nothing but the edge points dividing the unit interval I into I_1 and I_2 as described in Section 3. The adjacency matrix is given by H_1 in Section 3. The topological entropy is obtained from the logarithm of the largest eigenvalue of the adjacency matrix, which is explicitly given by $\log \frac{1+\sqrt{5}}{2}$. The above two subintervals construct the least division to obtain the topological entropy. The output degree distribution is given by $P(d) = \frac{1}{2}\delta_{d,1} + \frac{1}{2}\delta_{d,2}$.

The period-4 UPOs satisfying $x = R^3L(x)$ is given by $x = 2/9$, $L(2/9) = 13/18$, $RL(2/9) = 5/9$ and $R^2L(2/9) = 8/9$. The initial value $x = 2/9 + \epsilon/2^3$ $(0 < \epsilon \ll 1)$ is mapped to $R^3L(2/9+\epsilon/2^3) = 2/9-\epsilon$. We choose the initial value $x^* \in [2/9-\epsilon/2^3, 2/9+\epsilon/2^3]$. The four points $x = x^*$, $L(x^*)$, $RL(x^*)$, $R^2L(x^*)$ with the edge points $x = 0, 1$ and the boundary point $x = 1/2$ divide the unit interval into six subintervals. The adjacency matrix is given by

$$\begin{pmatrix} 0&0&0&0&0&1 \\ 0&0&0&0&1&0 \\ 1&0&0&0&1&0 \\ 1&0&0&1&0&0 \\ 0&1&0&1&0&0 \\ 0&1&1&0&0&0 \end{pmatrix},$$

from which the topological entropy is obtained as $\log \frac{1+\sqrt{5}}{2}$. The output degree distribution is given by $P(d) = \frac{1}{3}\delta_{d,1} + \frac{2}{3}\delta_{d,2}$.

The period-5 UPOs satisfying $x = R^4L(x)$ is given by $x = 2/15$, $L(2/15) = 19/30$, $RL(2/15) = 11/15$, $R^2L(2/15) = 8/15$ and $R^3L(2/15) = 14/15$. The initial value $x = 2/15 + \epsilon/2^4$ $(0 < \epsilon \ll 1)$ is mapped to $R^4L(2/15 + \epsilon/2^4) = 2/15 + \epsilon$. We choose the initial value $x^* \in [2/15 - \epsilon/2^4, 2/15 + \epsilon/2^4]$. The five points $x = x^*$, $L(x^*)$, $RL(x^*)$, $R^2L(x^*)$, $R^3L(x^*)$ with the edge points $x = 0, 1$ and the boundary point $x = 1/2$ divide the unit interval into seven subintervals. The adjacency matrix is given by

$$\begin{pmatrix} 0&0&0&0&0&0&1 \\ 0&0&0&0&0&1&0 \\ 1&0&0&0&0&1&0 \\ 1&0&0&0&1&0&0 \\ 0&1&0&0&1&0&0 \\ 0&1&0&1&0&0&0 \\ 0&1&1&0&0&0&0 \end{pmatrix},$$

from which the topological entropy is obtained as $\log \frac{1+\sqrt{5}}{2}$. The output degree distribution is given by $P(d) = \frac{3}{7}\delta_{d,1} + \frac{3}{7}\delta_{d,2} + \frac{1}{7}\delta_{d,3}$.

The convergence of the numerical procedure described in Section 5 is measured by the topological entropy. In the case of the above-mentioned UPOs, the topological entropies coincide with each other. In general, the topological entropy is assumed to converge with the exact value, as the period of approximately obtained UPO becomes long enough. We see from the above example that the topological entropy is obtained from the least subintervals and is also obtained from other redundant subintervals. There exist an infinite variation of adjacency matrices and the directed graphs corresponding to the single topological entropy. In the case of the above example, the output degree distribution $P(d)$ is slightly fluctuating around $P(d) = \frac{1}{2}\delta_{d,1} + \frac{1}{2}\delta_{d,2}$ for the least division. The output degree distribution is assumed to fluctuate slightly around a fixed distribution, as the period of approximately obtained UPO becomes long enough and the topological entropy converges with a fixed value.

Starting from a matrix representation H_q of the generalized Frobenius-Perron operator $\mathcal{H}_q$ related to large-deviation statistics of the local expansion rate, we regard H_1 as a adjacency matrix and construct a directed graph. Nodes of this directed graph can be related to some finite UPOs among the countable infinite number of UPOs, which is a description of chaos induced by a one-dimensional map as an irregular switching between some finite specific UPOs. Some characteristics of bifurcations appear network statistics of the above-mentioned directed graph constructed from H_1. In this study, we focus on Type-I intermittency caused by tangent bifurcation. It is a future problem to make clear such network statistics for other bifurcations such as band crisis or modulational intermittency also known as on-off intermittency. Various network statistics other than output degree distribution will be considered.

Acknowledgments. This work was supported by a Grant-in-Aid for Scientific Research (c) (No. 20540376).

References

Bollt, E., Lai, Y.-C. and Grebogi, C. (1997) Coding, channel capacity, and noise resistance in communicating with chaos, *Phys. Rev. Lett.*, **79**, 3787–3790.

Fujisaka, H. and Inoue, M. (1987) Theory of diffusion and intermittency in chaotic systems. III, *Prog. Theor. Phys.*, **78**, 268–281.

Fujisaka, H. and Shibata, H. (1991) New asymptotic law governing overall temporal correlations in chaotic systems, *Prog. Theor. Phys.*, **85**, 187–204.

Gaspard, P. (1998) *Chaos, Scattering and Statistical Mechanics*, Cambridge University Press, U.K.

Mori, H. and Kuramoto, Y. (1998) *Dissipative Structures and Chaos*, Springer, Germany.

Shobu, K., Ose, T. and Mori, H. (1984) Shapes of the power spectrum of intermittent turbulence near its onset point, *Prog. Theor. Phys.*, **71**, 458–473.

Zhang, J. and Small, M. (2006) Complex network from pseudoperiodic time series: Topology versus dynamics, *Phys. Rev. Lett.*, **96**, 238701-1–238701-4.

Zhang, J., Sun, J., Luo, X., Zhang, K., Nakamura, T. and Small, M. (2008) Characterizing pseudoperiodic time series through the complex network approach, *Physica D*, **237**, 2856–2865.